Reaction of Hydrogen Gas with C_{60} at Elevated Pressure and Temperature: Hydrogenation and Cage Fragmentation†

Alexandr V. Talyzin,*,‡ Yury O. Tsybin,§ Jeremiah M. Purcell,§,# Tanner M. Schaub,§ Yury M. Shulga,|| Dag Noréus,⊥ Toyoto Sato,⊥ Andrzej Dzwilewski,‡ Bertil Sundqvist,‡ and Alan G. Marshall§,#

Department of Physics, Umeå University, 901 87 Umeå, Sweden, Ion Cyclotron Resonance Program, National High Magnetic Field Laboratory, Tallahassee, Florida 32310-4005, Department of Chemistry and Biochemistry, Florida State University, Tallahassee, Florida 32306, Institute of Problems of Chemical Physics, RAN, 142432 Chernogolovka, Moscow Region, Russia, and Department of Structural Chemistry, Stockholm University, Stockholm, Sweden

Received: October 11, 2005; In Final Form: January 9, 2006

Products of the reaction of C_{60} with H_2 gas have been monitored by high-resolution atmospheric pressure photoionization Fourier transform ion cyclotron resonance mass spectrometry (APPI FT-ICR MS), X-ray diffraction, and IR spectroscopy as a function of hydrogenation period. Samples were synthesized at 673 K and 120 bar hydrogen pressure for hydrogenation periods between 300 and 5000 min, resulting in the formation of hydrofullerene mixtures with hydrogen content ranging from 1.6 to 5.3 wt %. Highly reduced $C_{60}H_x$ ($x >$ 36−40) and products of their fragmentation were identified in these samples by APPI FT-ICR MS. A sharp change in structure was observed for samples with at least 5.0 wt % of hydrogen. Low-mass (300−500 Da) hydrogenation products not observed by prior field desorption (FD) FT-ICR MS were detected by APPI FT-ICR MS and their elemental compositions obtained for the first time. Synthetic and analytical fragmentation pathways are discussed.

Introduction

Hydrofullerenes are products of C_{60} reaction with hydrogen. Starting from the simplest hydrofullerene $C_{60}H_2$,[1] many hydrofullerenes, $C_{60}H_x$, with various numbers of hydrogen atoms, $2 < x < 44$, have been synthesized.[2−6] Hydrogen reaction with C_{60} occurs by addition of H_2 at a C═C double bond, which results in formation of two C−H bonds. Therefore, only an even number of hydrogen atoms is expected in neutral $C_{60}H_x$ molecules. Of the several methods reported for synthesis of hydrofullerenes, the most important are Birch reduction,[2] reaction with molten dihydroanthracene (transfer hydrogenation),[3] and reduction by zinc and hydrochloric acid.[4] Typically, the two most abundant hydrofullerene molecules from these reactions are $C_{60}H_{18}$ and $C_{60}H_{36}$ and, consequently, most hydrofullerene studies have been limited to those products. Numerous characterization methods (X-ray diffraction (XRD), NMR, IR, Raman spectroscopy, etc.)[7−10] have been employed to characterize those products. The high selectivity in synthesis of $C_{60}H_{36}$ is explained by an inability of the above-mentioned synthesis methods to reduce unconjugated double bonds (e.g., the minimum number of hydrogen atoms required to leave unconjugated double bonds in each of the pentagons of C_{60} is 36). Recently, it was discovered that hydrofullerenes of the type $C_{60}H_x$ with $x = 38-44$ can be synthesized by a Benkeser reduction (reduction by lithium in ethylenediamine).[11] Highly reduced C_{60} (with more than 44 hydrogen atoms attached) has never been obtained in solid state.

Until recently, there were relatively few reports of C_{60} reacting directly with hydrogen gas. That reaction requires elevated temperature (∼573−673 K) and a hydrogen pressure of 50−120 bar and yields mixtures of hydrofullerenes with variable composition.[12−16] The resultant mixture is rather complex, and simple characterization methods (such as IR spectroscopy and XRD) cannot speculate on the reaction products. The maximum overall hydrogen content achieved after prolonged hydrogenation (at 673 K and 100 bar H_2) is ∼5 wt %. Upon prolonged hydrogenation, the sample weight initially increases due to hydrogen addition and after reaching some maximum, starts to decrease due to partial cage collapse.[16] We recently showed that the final products of C_{60} collapse are likely polycyclic aromatic hydrocarbons (PAH).[16,17] Surprisingly, not only collapse but also fragmentation of the cage structure was found under conditions of prolonged hydrogenation. In our previous study, we reported synthesis of $C_{59}H_x$ and $C_{58}H_x$ as major products after hydrogenation at elevated temperature/pressure:[18] two samples with relatively high degree of hydrogenation were analyzed by high-resolution field desorption Fourier transform ion cyclotron resonance mass spectrometry (FD FT-ICR MS). However, such analysis destroys highly unstable hydrofullerene molecules (highly reduced C_{56-60}). Therefore, a complementary method is required for analysis of "superhydrogenated" samples. Furthermore, FD FT-ICR MS was performed only on highly reduced samples and the degree of hydrogenation required for the onset of fragmentation (from $C_{60}H_x$ to $C_{56-59}H_x$) was unknown.[18,19]

Here we present a systematic analysis of samples synthesized by reaction of C_{60} with H_2 gas. By variation of the hydrogenation period, samples with a broad range of hydrogen content (1.4−5.3 wt %) could be synthesized. The complex hydrofullerene mixtures were studied by IR spectroscopy, XRD and high-resolution atmospheric pressure photoionization Fourier trans-

† Part of the "Chava Lifshitz Memorial Issue".

* Corresponding author. E-mail: alexandr.talyzin@physics.umu.se.
‡ Umeå University.
§ National High Magnetic Field Laboratory.
# Florida State University.
|| Institute of Problems of Chemical Physics.
⊥ Stockholm University.

10.1021/jp0557971 CCC: $33.50
Published on Web 02/23/2006

form ion cyclotron resonance mass spectrometry (APPI FT-ICR MS). The recently developed APPI FT-ICR MS method[20] has been employed for the first time for analysis of hydrogenated fullerenes and shows promise as less destructive than FD FT-ICR MS.

Experimental Section

C_{60} powder (0.5−1 g, 99.5% pure, MTR Ltd., Cleveland, OH) was typically loaded in an alumina container. Hydrogenation at 120 bar H_2 gas pressure, 673 K was performed for periods of 300−5000 min. Prior to hydrogenation the system was flushed with hydrogen at room temperature and degassed by heating to 473 K in a vacuum for several hours. The samples were degassed by heating at 473 K in a vacuum (10^{-5} Torr) for several hours. Hydrogenation was performed with an apparatus consisting of an alumina container inserted in a steel autoclave connected to a hydrogen pressure system. A stainless steel sealed thermocouple was in a direct contact with the sample to control the sample temperature during the reactions. In total, seven powder samples were synthesized and analyzed by powder XRD, Raman and IR spectroscopy. The final C/H composition of the samples was determined from elemental analysis by flash combustion gas chromatography (FC GC) (Mikro Kemi AB, Uppsala, Sweden). Briefly, concerning the FC GC method, the samples are first dried under vacuum, then completely oxidized into gaseous CO_2 and H_2O and subsequently analyzed by gas chromatography. Gas concentration is determined by thermal conductivity and the accuracy of the hydrogen analysis is estimated to be ±0.1%.

Hydrogen composition analysis revealed that the hydrogenation period did not consistently result in the same C/H ratio. Some deviation in time dependence could be explained by slight contamination with metal alloy particles (the same apparatus was routinely used for work with hydrogenation of metal alloys). The rate of hydrogenation depends strongly on powder grain size, size of used containers, and purity of hydrogen. Therefore, in the following discussions the samples will be denoted not by the hydrogenation period but according to the degree of their hydrogenation determined from C/H analysis confirmed by XRD and IR.

IR spectra were collected with a Perkin-Elmer Spectrum BX-II spectrometer for powder samples pressed in a KBr pellet. The X-ray powder diffraction analysis was performed by use of the Cu Kα line from a Philips powder diffraction system with a PW1820 goniometer.

High-resolution mass spectrometry was performed with 9.4 T Fourier transform ion cyclotron resonance mass spectrometers equipped with atmospheric pressure photoionization[21] and field desorption/ionization[22] sources. Samples were dissolved in toluene and either delivered at a flow rate of 100 μL/min into the APPI ion source or deposited in 20−40 nL amounts on the filament emitter of the FD ion source in vacuo. The nebulizing gas was supplied to the APPI ion source at 80 psi and the nebulizer temperature was operated in the range of 200−350 °C. APPI produces both radical cations (loss of an electron) and protonated cations. Radical ion formation in the APPI source results from 10 eV photons emitted by a krypton vacuum UV lamp or charge exchange reactions with toluene cations, whereas protonated cations are formed via proton-transfer reactions with toluene cations.[23] The generated ions were accumulated in an external (to the magnetic field) octopole ion trap for 0.1−2 s prior to injection into an open cylindrical Penning ion trap located in a homogeneous 9.4 T magnetic field. Trapped ions were excited and detected following standard procedures described elsewhere.[21] To increase signal/noise ratio, transient time-domain ICR signals were summed prior to fast Fourier transformation and magnitude calculation. The experimental event sequence for the FD FT-ICR MS experiment has previously been described in detail.[19]

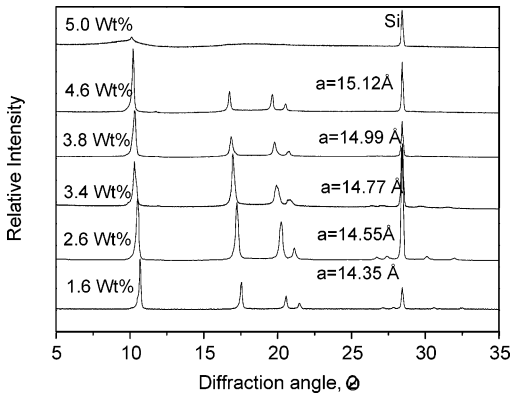

Figure 1. X-ray diffraction patterns recorded from samples of C_{60} with different degrees of hydrogenation (shown as weight percent of hydrogen for each sample). The cell parameter *a* calculated for a FCC structure is shown for several samples. Silicon powder was used as an internal standard.

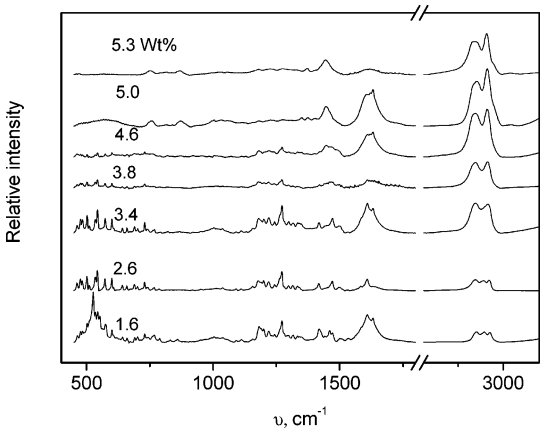

Figure 2. Infrared absorption spectra of samples with different degrees of hydrogenation.

Results and Discussion

X-ray Diffraction Characterization. Figure 1 shows XRD patterns recorded from samples with different degrees of hydrogenation. Under normal conditions (room temperature, atmospheric pressure), the C_{60} crystal structure is face-centered cubic (FCC) with a cell parameter, $a = 14.17$ Å.[24] The structure of hydrogenated C_{60} remains the same, but the cell parameter increases in proportion to the degree of hydrogenation up to $a = 15.12$ Å for the sample with 4.6 wt % of hydrogen. Stronger hydrogenation results in amorphization of the structure. Some low-amplitude peaks were still observed for the sample with 5 wt % of hydrogenation, whereas the sample with the strongest hydrogenation (5.3 wt %, not shown in Figure 1) was completely amorphous with only some very broad and weak features instead of diffraction peaks. This result is in good agreement with our previous data show that ∼5 wt % is a stability limit for C_{60} hydrofullerenes.

IR Spectroscopy Characterization. Figure 2 shows IR spectra recorded from samples with different degree of hydrogenation. The IR spectra of hydrogenated fullerenes exhibit cage vibrations (<1700 cm^{-1}) and C−H vibrations (∼2700−3000 cm^{-1}). Figure 2 shows some clear modifications in both spectral

TABLE 1: Peak Positions for C−H Vibrations from the IR Spectra Recorded on Hydrofullerene Samples with Different Degrees of Hydrogenation (Compared to Literature Data for $C_{60}H_{18}$[15] and $C_{60}H_{36}$[25])

wt %						
1.6		2851	2877	2896	2928	
2.6		2847	2882	2897	2925	
3.4		2845		2895	2922	
3.8	2832	2857		2897	2917	
4.6	2828	2859			2913	
5.0	2831	2861			2913	2948
5.3	2826	2858			2909	2946
$C_{60}H_{18}$[15]		2847			2920	
$C_{60}H_{36}$[25]	2829	2849			2911	

regions upon increased degree of hydrogenation. In agreement with the XRD data of Figure 1, a strong change is observed for highly reduced samples (5 and 5.3 wt %). According to our previous data and in agreement with XRD data shown above, partial collapse of the cage structure begins for samples with ~5 wt % of hydrogen content and higher. New peaks at 751, 810, 837, 866, 1179, 1123, 1274, 1369, and 1444 cm^{-1} are found in both the 5 and 5.3 wt % spectra (Figure 2) and can be attributed to modified cage vibrations. The region of fullerene C−H vibrations shows peaks at 2831, 2861, 2913, 2948 cm^{-1} (for the 5 wt % sample); see also Table 1. Also some broad weaker peaks centered at approximately 3020 and 3044 cm^{-1} are found in the spectral region typically indicative of valence C−H vibrations for aromatic compounds and PAH. As suggested earlier, those peaks are due to partial collapse of cage structure with formation of relatively large hydrocarbon fragments of $C_{60}H_x$.[19]

Samples with lower hydrogen content (≤4.6 wt %) are composed of hydrofullerenes with different numbers of hydrogen atoms. Precise identification of all $C_{60}H_x$ species in these samples from IR spectroscopy is not possible because each sample is a complex mixture of many hydrofullerenes. The literature data on IR spectroscopy provides information for the two most studied materials: $C_{60}H_{36}$ and $C_{60}H_{18}$. Although those hydrofullerenes were isolated in a reasonably pure state, precise analysis is difficult due to large number of possible isomers. The $C_{60}H_{18}$ species can be confidently identified as a main component of the 2.6 and 3.4 wt % samples (see Figure 2). Several sharp peaks, often overlapped, are in good agreement with data provided by Darwish et al. for $C_{60}H_{18}$.[15]

The agreement is also good for C−H vibrations (see Table 1). The most distinct peaks for the 3.4 wt % sample are found at (asterisk marks the data from ref 15): 463 (463*), 476 (476*), 484 (484*), 502 (502*), 510, 534 (535*), 543 (544*), 573 (574*), 600 (601*), 606, 641, 659, 689, 702, 730, 740, 767, 1180 (1179), 1189, 1120, 1243 (1243*), 1265, 1272 (1272*), 1298, 1316, 1333, 1340, 1348, 1418, 1442, 1450, 1471 (1471*), and 1500 cm^{-1}. The $C_{60}H_{18}$ composition corresponds to hydrogen content of ~2.4 wt %. Therefore, it is not surprising that most of the 2.6 wt % sample (Figure 2) can be assigned to $C_{60}H_{18}$. IR spectra from samples with less hydrogen (1.6 wt %) also contain some peaks from $C_{60}H_{18}$, as well as some peaks from other hydrofullerenes. Besides peaks assigned to $C_{60}H_{18}$, some unidentified peaks (probably from hydrofullerenes with number of hydrogen below 18) were found at 526, 552, 789, 819, 830, 860, 1200, 1220, 1426, and 1460 cm^{-1}. Peaks due to C−H vibrations were also found at somewhat different positions (see Table 1). Finally, the color of the 1.6 wt % sample is black (whereas other samples are red or orange) and solubility in toluene was much lower.

The 4.6 wt % hydrogen content corresponds approximately to the composition of $C_{60}H_{36}$, which is the most studied hydrofullerene. Indeed, peaks due to C−H vibrations found for samples with 4.6 and 3.8 wt % are similar to those described for $C_{60}H_{36}$.[25] No clear signatures for $C_{60}H_{36}$ can be found in the cage vibration regions. Many of the sharp peaks observed for these two samples below 1600 cm^{-1} are exactly the same as peaks from samples with less hydrogen content, $C_{60}H_{18}$, but less intense. All observed peaks in this region are broader and less intense, which typically are the attributes of complex sample composition. From the IR data, the nature of the 4.6 wt % sample cannot be explained by suggesting that most of the sample consists of $C_{60}H_{36}$ species, as might be inferred from the high abundance of this particular hydrofullerene in samples obtained by different chemical reduction methods. Nevertheless, a high degree of hydrogenation is confirmed by similarity of peaks from C−H vibrations to those observed in $C_{60}H_{36}$.

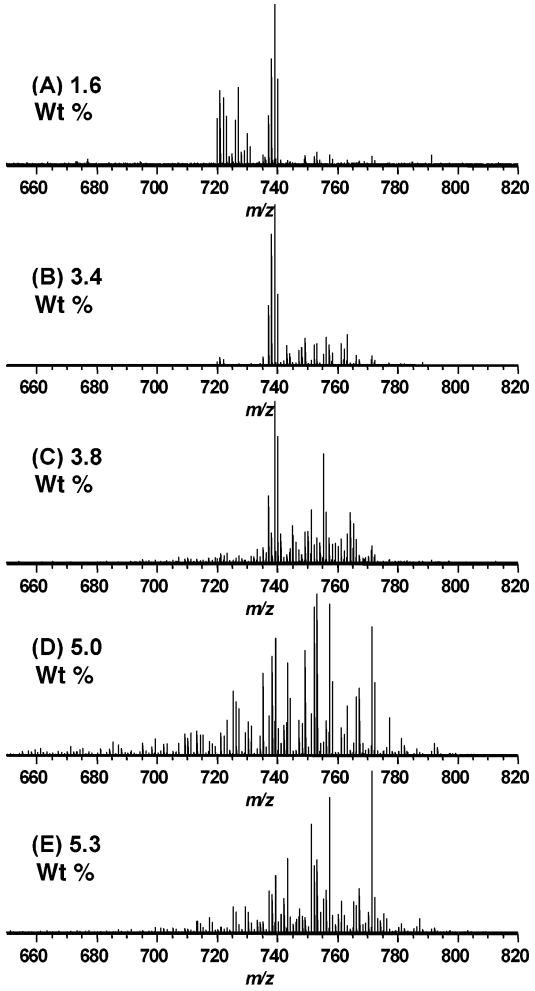

Figure 3. APPI FT-ICR mass spectra of C_{60} samples with different degrees of hydrogenation.

It is clear that IR spectroscopy can be used as a tool to estimate degree of hydrogenation and to identify some hydrofullerenes ($C_{60}H_{18}$ in our case) if they compose the major part of the sample, but the method cannot distinguish elemental compositions in complex mixtures of hydrofullerene materials. For that purpose, high-resolution mass spectrometry is required.

APPI FT-ICR MS of Hydrogenated Samples. High-resolution APPI FT-ICR mass spectra were recorded from five samples of C_{60} with different degrees of hydrogenation (Figure 3) and a non-hydrogenated reference C_{60} sample (data not shown). Note that prior to analysis, the samples were dissolved in toluene and only molecules soluble in that solvent will be detected. Due to the difference in solubility for different

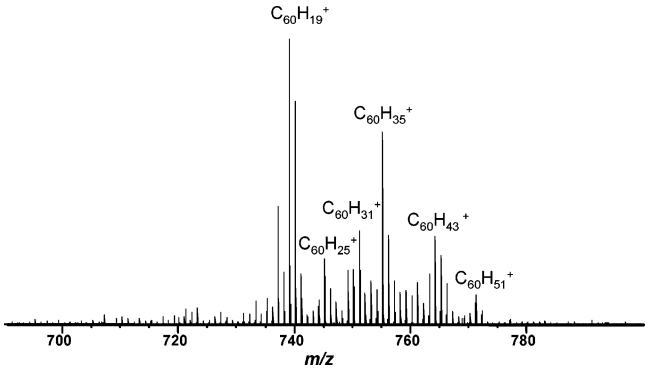

Figure 4. APPI FT-ICR MS from the 3.8 wt % sample. The most abundant ions are assigned.

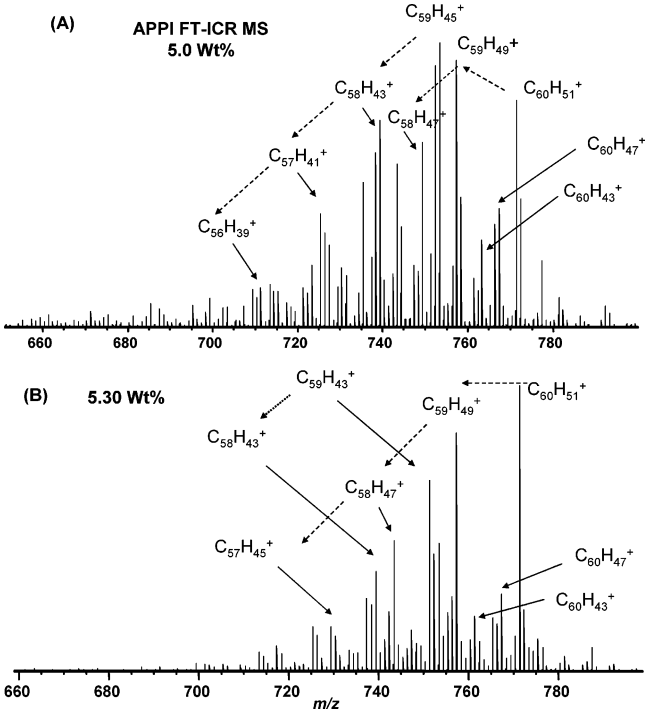

Figure 5. APPI FT-ICR mass spectra from the samples with maximum hydrogenation (5.0 and 5.3 wt %).

hydrofullerenes as well as differences in ionization efficiency, the relative ion abundances in the mass spectrum may not correlate to the abundances of the corresponding neutral synthesized hydrofullerenes. The ultrahigh resolution and ultrahigh mass accuracy of FT-ICR MS[26] allow for the unique elemental composition assignment of each peak in a complex mass spectrum.[27]

APPI FT-ICR mass spectra of pure C_{60} and low hydrogen content (1.6 and 2.6 wt %) hydrofullerene mixtures demonstrated the presence of only $C_{60}H_x$ species with no fragmented fullerenes. The 1.6 wt % sample consists mostly of $C_{60}H_{18}$, $C_{60}H_{10}$, $C_{60}H_6$ and C_{60}. Most likely, hydrofullerenes with 2−10 hydrogens are less soluble in toluene; thus their concentration in the initial powder is likely much higher than the corresponding relative ion abundances in Figure 3. Note that the 1.6 wt % sample was much less soluble than other samples. In good agreement with IR spectroscopy data (Figure 2), MS analysis of 2.6 wt % (data not shown) and 3.4 wt % (Figure 3 b) samples shows that they are composed mostly of $C_{60}H_{18}$ (observed as protonated $[C_{60}H_{18} + H]^+$). The most abundant ions in Figure 3b for 3.4 wt % sample can be interpreted as protonated molecules originating from $C_{60}H_{24}$, $C_{60}H_{30}$, $C_{60}H_{34}$, $C_{60}H_{42}$ and

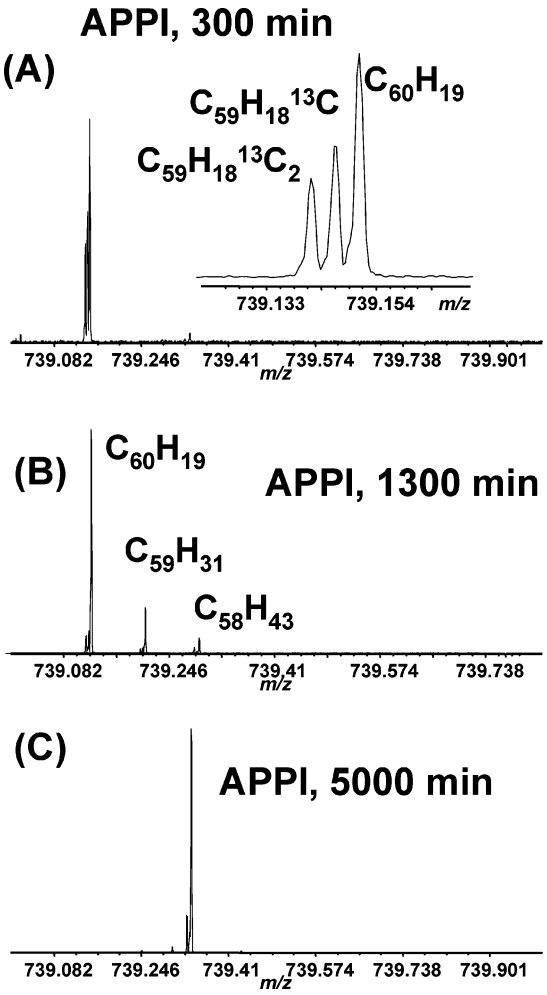

Figure 6. Scale-expanded *m/z* segment, 739−740 Da, for samples with different hydrogen contents.

$C_{60}H_{50}$. An increase in the degree of hydrogenation to 3.8 wt % results in a significant increase in relative abundances of ions with hydrogen numbers $x > 24$, especially for $C_{60}H_{34}$ molecular ions ($[C_{60}H_{34} + H]^+$); see Figure 4. Moreover, some low-abundance ions from $C_{59}H_x$ and $C_{58}H_x$ with $x > 28$ appear.

Fragmentation increases markedly in the samples hydrogenated to 5.0 and 5.3 wt % (Figure 5). Major peaks in the spectrum of the 5.3 wt % sample are from highly hydrogenated C_{60} with hydrogen numbers above 40, with the highest relative abundance for $C_{60}H_{51}^+$ ions (Figure 5b). The most abundant fragmented fullerenes seem to follow two different pathways. Several signals can be explained by CH_2 loss from $C_{60}H_{51}^+$ ions, whereas some others, for example, $C_{59}H_{43}^+$ and $C_{58}H_{43}^+$, differ by the mass of one carbon.

The most important question arising from Figure 5 is how to relate a mass spectrum to the chemical composition of the sample: is the fragmentation reaction a result of instrument-induced effects or are fragmented hydrofullerenes the result of synthesis? It is clear that more than one mechanism of fragmentation can be deduced from Figure 5a,b, and the data analysis is further complicated by formation of both radical cations and protonated molecules.

Mass scale-expanded segments demonstrate the resolved isotopic cluster and increased abundance of fragmented fullerene ions ($C_{58}H_{43}^+$ and $C_{59}H_{31}^+$) generated from samples with higher hydrogen content (Figure 6). The absence of ions originating

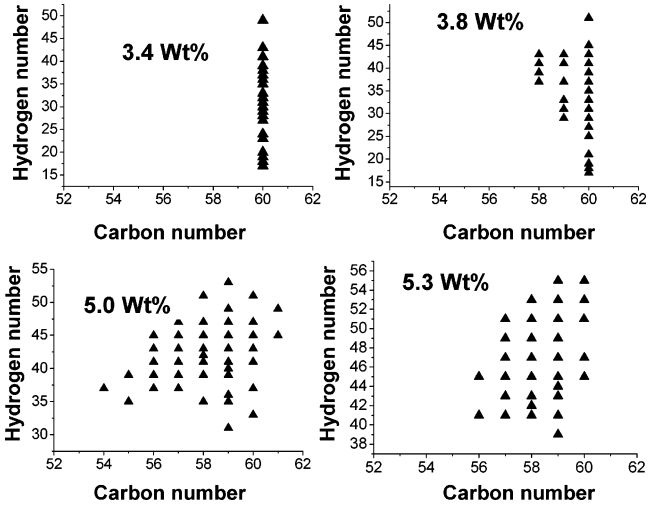

Figure 7. Carbon and hydrogen compositions obtained from APPI FT-ICR mass spectra (for mass spectral peaks with S/N > 7).

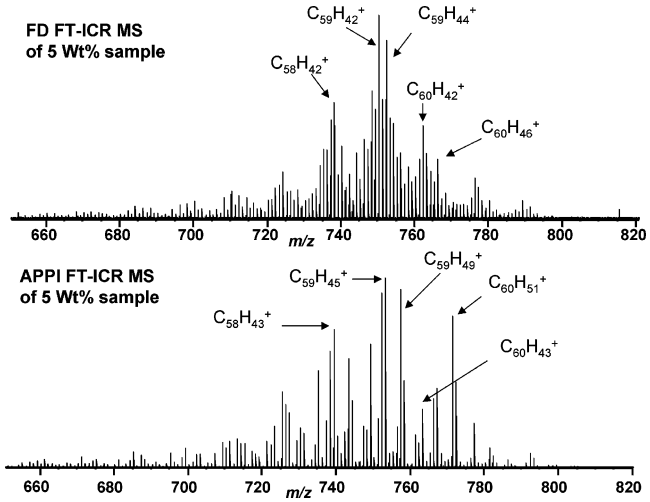

Figure 8. FT-ICR mass spectra of 5.0 wt % samples: (top) FD; (bottom) APPI.

from the $C_{60}H_{18}$ molecule ($[C_{60}H_{18} + H]^+$) in the high hydrogen content sample is due to higher degree of hydrogenation during synthesis.

Elemental compositions were assigned for all APPI FT-ICR mass spectra obtained from samples with different degrees of hydrogenation. The results of such analysis are shown in Figure 7. Fragmentation is clearly observed only for hydrofullerenes with a high number of hydrogen atoms (more than 28). That observation is in good agreement with our previous FD FT-ICR MS results.[19] The second observation is the chain of fragmentation products is not long: no hydrofullerenes with fewer than 54 carbons were observed. The presence of ions with composition $C_{61}H_x$ is most likely explained by addition of CH_2 ions formed during fragmentation of some molecules. Similar addition of C_2 units was observed during fragmentation of pure C_{60} by a C_2 loss mechanism.[28] Interestingly, the longest chain of fragmentation is not observed for the sample with the highest degree of hydrogenation (see also Figure 5). Also note that the most abundant ions for the 5.0 wt % sample originate from $C_{59}H_x$ with $x \sim 44-48$, whereas for the sample with the highest degree of hydrogenation they originate from $C_{60}H_{50}$ by formation of $[C_{60}H_{50} + H]^+$. The increased amount of highly hydrogenated ions ($[C_{60}H_{50} + H]^+$) is in a good agreement with stronger hydrogenation of this sample.

APPI versus FD FT-ICR MS. The 5 wt % sample was also analyzed by FD FT-ICR MS and the results are compared to the APPI mass spectrum in Figure 8. The mass scale-expanded segments of similar mass spectra demonstrating resolved isotopic patterns can be found in the inset of Figure 6a of the present paper (APPI) and in Figure 4 of the previous publication (FD).

Conditions for the FD FT-ICR mass analysis were optimized to minimize fragmentation. Indeed, the chain of fragmentation products is much shorter in Figure 8 compared to our previously published spectra for a sample of similar hydrogen content. [19]

The two mass spectra in Figure 8 demonstrate some general similarity but also major differences in relative ion abundances. For APPI FT-ICR MS, the presence of mostly odd number of hydrogens, x, in $C_{60}H_x$ is explained by the dominance of protonation over radical cation formation. The most abundant ions in both mass spectra are $C_{59}H_x$: the FD mass spectrum shows maximum abundance for species with 42 and 44 hydrogen atoms, whereas the APPI mass spectrum has a maximum at 44 (taking into account that one hydrogen in APPI MS is from protonation). Similarly, good agreement is observed for C_{58} hydrofullerene ions. Note that "parent" ions from $C_{60}H_{42-44}$ are present in both spectra and show similar abundances relative to fragmentation products.

The most prominent difference between the two observations is for $C_{60}H_x$ with $x > 50$. The APPI mass spectrum shows a very high-magnitude peak corresponding to $[C_{60}H_{50} + H]^+$ ions, whereas the corresponding species in the FD mass spectrum is much lower in abundance. The APPI mass spectrum also shows major peaks from ions likely produced as a result of $[C_{60}H_{50} + H]^+$ fragmentation by a CH_2 loss mechanism (see Figure 5b).

We propose the following interpretation of the data shown in Figures 5−7. Some of the fragmented fullerenes $C_{58}H_x$ and $C_{59}H_x$ are produced during synthesis after prolonged hydrogenation periods, as previously proposed.[19] That is why the most abundant ions in both FD and APPI FT-ICR mass spectra originate from $C_{59}H_{42-44}$ molecules. Instrument-induced fragmentation is relatively weak in our new optimized experiments (Figure 7) for ions with fewer than 44 hydrogen atoms but is seen for ions with a higher number of hydrogen atoms. For example, $[C_{60}H_{50} + H]^+$ ions in Figure 7 undergo fragmentation by CH_2 loss. Note that this mechanism (CH_2 loss) is clearly different from that observed by FD FT-ICR MS (in which fragmentation occurred by loss of C_2H_2 units[19]). The difference is most likely due to specific features of each method: different ionization mechanism/ions, different pressure and temperature conditions.

Low-Mass Ions. APPI mass spectra of samples with 5 and 5.3 wt % also exhibit low-mass ions, $300 < m/z < 600$. Most likely these ions form hydrocarbon molecules as a result of C_{60} cage collapse. Partial collapse of hydrofullerenes during prolonged hydrogenation was reported in our previous publications, but analysis of fullerene fragments was limited to IR spectroscopy and low-resolution matrix assisted laser desorption/ionization time-of-flight mass spectrometry (MALDI TOF MS).[17] Because the sample synthesis was performed under conditions of carbon−hydrogen reaction, relatively large fullerene fragments terminated by hydrogen atoms could survive from the collapse. Most likely, these molecules consist of hexagons and pentagons, but rings with seven and eight carbons could appear as previously discussed.[16]

An APPI mass spectrum recorded with instrumental parameters that provide significant enhancement of sensitivity in the low-mass region is shown in Figure 9. In general, the mass spectrum shows very good agreement with MALDI TOF mass spectra obtained previously for one of HPLC fractions separated

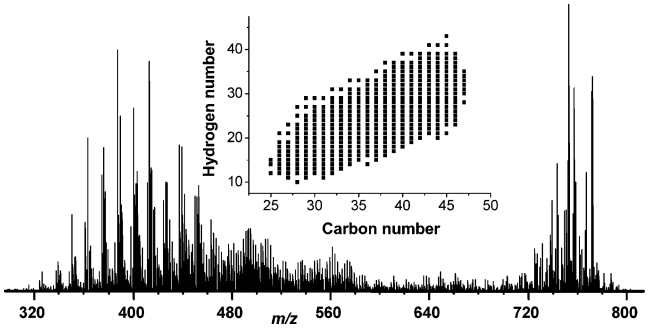

Figure 9. APPI FT-ICR MS of the 5.3 wt % sample under conditions that favor higher abundance of low-mass ions. Filled triangles denote higher-abundance species.

from a highly hydrogenated sample. The common feature of these mass spectra is a sharp reduction in abundance of ions with molecular weight below ~350 Da. Because the synthesis of this sample was performed at high temperature (673 K), all light hydrocarbons with low melting points (and high vapor pressures) had evaporated. Preserved hydrocarbons show a broad distribution of different compositions with a maximum near ~380−420 Da and the highest abundance for $C_{31}H_{15}^+$. In general, the highest abundance is observed for the ions with an approximate carbon/hydrogen ratio of 2:1 (Figure 9, inset).

IR spectra recorded from this sample (Figure 2) show some specific features in the region typically associated with C−H vibrations of polycyclic aromatic hydrocarbons (PAH). Perhaps some of the peaks shown in Figure 9 originate from flat molecules. It is also likely that collapse of C_{60} forms fragments with both pentagons and hexagons in the structure. In that event, molecules with some curvature must form. "Bowl-like" molecules similar to corannulene ($C_{20}H_{10}$)[29] but of a larger size are probably a significant part of the studied sample.

Elemental Composition of Hydrofullerene Mixtures. Considering the remarkably high stability and selectivity of $C_{60}H_{18}$ and $C_{60}H_{36}$ molecules during synthesis by chemical reduction methods, one might anticipate that reaction of C_{60} with H_2 gas would also lead to formation of relatively high amounts of $C_{60}H_{18}$ and $C_{60}H_{36}$. That prediction appears to be only partly true: both IR spectroscopy and APPI FT-ICR MS show high selectivity for the synthesis of $C_{60}H_{18}$ (hydrogen composition for the $C_{60}H_{18}$ compound is estimated to be ~2.4 wt %) only on the initial stages of hydrogenation. In fact, the toluene-soluble portion of the samples with 2.6 and 3.4 wt % of hydrogen appears to be essentially pure $C_{60}H_{18}$ (see Figure 3 for 3.4% sample analysis). That result is especially interesting because $C_{60}H_{36}$ (~4.76 wt % of hydrogen) was not especially abundant in samples with higher degree of hydrogenation. That composition ($C_{60}H_{36}$) is limiting for several hydrogenation methods; for example, Birch reduction does not produce any hydrofullerenes with a higher number of hydrogen atoms.[2] For high-temperature reaction of C_{60} with hydrogen gas, the limitation is obviously not valid and hydrofullerenes with hydrogen atom numbers up to ~52−56 are formed. IR spectra of these complex mixtures are devoid of sharp peaks and show only broad and poorly resolved features (Figure 2). These highly hydrogenated species are less stable and mass spectrometric analysis of samples that contain $C_{60}H_x$ with $x > 36$ is complicated by significant fragmentation induced during mass analysis. Remarkably, the fragmentation mechanism observed by APPI FT-ICR MS (loss of CH_2 units) is different from the dominant C_2H_2 loss previously reported for FD FT-ICR MS.[19] A similar fragmentation mechanism was previously reported for $C_{60}H_{36}$,[30] but the low resolution of their methods did not allow the exact determination of the number of hydrogen atoms in CH_x units. The true mechanism of CH_2 unit loss is not yet clear: obviously only C−H units are present in $C_{60}H_x$ molecules. The source of the second hydrogen atom and how the CH_2 units are formed will be a subject of future experiments. Probably the presence of not only radical cations but also protonated molecules in APPI MS can lead to a different fragmentation pathway.

In our prior studies, we also suggested that some fragmentation with loss of CH units could occur during the synthesis of hydrofullerenes under prolonged hydrogenation. Hydrogenated fragmented fullerenes, $C_{56-59}H_x$, are proposed to be present in our 5.0 and 5.3 wt % samples, but analysis of those fragmentation products is further complicated by fragmentation of highly reduced hydrofullerene ions during MS experiments.

As seen in Figure 5, the main fragment species are $C_{59}H_{43}^+$ and $C_{59}H_{49}^+$ (which correspond most likely to protonated $C_{59}H_{42}$ and $C_{59}H_{48}$). Both hydrofullerenes show their own set of fragmentation products differing by increments of CH_2. The $C_{59}H_{49}^+$ ion could be a fragmentation product from $C_{60}H_{51}^+$ originating from fragmentation during MS analysis.

Fragmentation during Hydrogenation. One of the possible mechanisms of hydrofullerene fragmentation during the hydrogenation process was discussed in our previous publications. In that model, highly reduced $C_{60}H_x$ species with $x > 40$ are not stable and can eject single carbon atoms (or more precisely, a CH unit). If a carbon atom is removed from a hexagon−pentagon edge, two bonds can re-form within the cage structure (forming a pentagon and 8-carbon ring) and formation of a dangling bond on the neighboring carbon atom that is then immediately saturated by a hydrogen atom. The mass change in such a process corresponds to one carbon atom. For example $C_{60}H_{44}$ could fragment to yield $C_{59}H_{44}$. Ejection of a neighboring carbon atom with a saturated dangling bond is most likely the next step of fragmentation, resulting in formation of a 7-carbon ring and a pentagon. The result of that two-step loss of two CH units will be $C_{58}H_{44}$. An ejected CH unit in this model must react with hydrogen gas to form CH_4. Removing the next two carbons will result in formation of a $C_{56}H_x$ structure, consisting of only hexagons and pentagons. This mechanism is similar to a well-known C_2 loss fragmentation described for pure C_{60}[31] and could lead to progressively smaller fullerene cages down to C_{28}. The only difference is C_2 loss from $C_{60}H_x$ is a two-step process that can result in the existence of odd numbered hydrofullerene cages as well.

An alternative suggestion is that re-forming of bonds within the cage structure does not occur and, once the carbon (or CH unit) is ejected, all three dangling bonds are immediately terminated by hydrogen atoms with formation of a hole. We believe that this variant is less likely because formation of a crown-like 11-carbon ring would be required.

A somewhat more "chemical" mechanism of C_{60} fragmentation can be considered. In that model, hydrogen attacks a C−C bond between two hydrogenated carbons. When that bond breaks, both carbon atoms expose dangling bonds terminated by hydrogen atoms. As a result, two CH_2 units, each connected to the cage by two C−C bonds, are formed. If that C−C bond breaks at a hexagon−pentagon junction, a nine-carbon ring with a hole in the cage structure will be formed. Next, a CH_2 unit may break from the cage, initiating re-formation of two dangling bonds into a C−C bond and formation of a pentagon. Alternatively, hydrogen attacks a C−C bond again and the hole size increases.

It is easy to see that both models lead to the same result but require a different number of steps. The main question remains

the same: can CH (or CH_2 in the second model) units be ejected from the cage accompanied by re-forming of remaining bonds in new C−C bond, or is the re-forming of C−C bonds prevented by immediate saturation with hydrogen atoms? Theoretical investigation is required to answer this question. It cannot be ruled out that temperature and pressure conditions of reaction can influence bond re-forming within a cage structure. Formation of a hole should be more likely at higher temperature and hydrogen pressure (dangling bonds are terminated by hydrogen before they join to each other). In that case, if a progressively larger hole is formed upon fragmentation, the process should stop at some point with collapse of the cage. Synthesis of small fullerene cages by progressive removal of carbon atoms in this mechanism is not possible.

Conclusion

In summary, XRD, IR spectroscopy, and high-resolution mass spectrometry serve to characterize the composition of samples obtained from C_{60} hydrogenation over a broad range of reaction periods. For the initial hydrogenation stages (hydrogen content in product molecules is less than 3 wt %) mostly $C_{60}H_{18}$ species are found. Increased hydrogenation period results in formation of hydrofullerenes with higher number of hydrogens, such as $C_{60}H_{36}$. Prolonged hydrogenation (formation of products with hydrogen content of ∼5 wt %) demonstrates the presence of highly reduced species ($C_{60}H_x$ with $x > 40$). Due to lower stability of hydrofullerenes with high hydrogen content, molecular ions from not only the highly reduced species but also from fragmented fullerenes $C_{54-59}H_x$ were observed in the mass spectra. The origin of the observed ions is not completely understood. Fragmentation of hydrofullerenes could occur during the synthesis and during mass spectrometric analysis. Unlike FD FT-ICR MS, fragmentation of hydrofullerene ions in APPI follows a CH_2 loss pathway. Nonetheless, we believe that some of the hydrogenated fullerenes with fragmented cages are formed during synthesis. Analysis of low mass ions (products of fullerene cage collapse) revealed abundant hydrocarbon molecules with carbon number of 25−45 and carbon number/hydrogen number ratio of 2/1.

The advent of APPI FT-ICR mass spectrometry for analysis of hydrofullerene mixtures presents several significant advantages over traditionally employed pulsed ionization techniques (electron impact ionization, field desorption and MALDI). Instrument-induced fragmentation in the APPI ion source should be minor relative to other ionization methods. Both radical and protonated cations are formed in the APPI ion source with the latter as the dominant ionization channel.

Acknowledgment. This work was supported by the NSF National High-Field FT-ICR Mass Spectrometry Facility (CHE-99-09502), Florida State University, and the National High Magnetic Field Laboratory in Tallahassee, FL. Y.M.S. thanks RFBR for support (project 06-03-32849). Part of the work was financially supported by the Swedish Research Council.

References and Notes

(1) Henderson, C. C.; Cahill, P. A. *Science* **1993**, *259*, 1885.
(2) Haufler, R. E.; Conceicao, J.; Chibante, L. P. F.; Chai, Y.; Byrne, N. E.; Flanagan, S.; Haley, M. M.; Obrien, S. C.; Pan, C.; Xiao, Z.; Billups, W. E.; Ciufolini, M. A.; Hauge, R. H.; Margrave, J. L.; Wilson, L. J.; Curl, R. F.; Smalley, R. E. *J. Phys. Chem.* **1990**, *94*, 8634.
(3) Ruchardt, C.; Gerst, M.; Ebenhoch, J.; Beckhaus, H. D.; Campbell, E. E. B.; Tellgmann, R.; Schwarz, H.; Weiske, T.; Pitter, S. *Angew. Chem., Int. Ed. Engl.* **1993**, *32*, 584.
(4) Darwish, A. D.; AbdulSada, A. K.; Langley, G. J.; Kroto, H. W.; Taylor, R.; Walton, D. R. M. *Synth. Met.* **1996**, *77*, 303.
(5) Kolesnikov, A. I.; Antonov, V. E.; Bashkin, I. O.; Grosse, G.; Moravsky, A. P.; Muzychka, A. Y.; Ponyatovsky, E. G.; Wagner, F. E. *J. Phys.−Condens. Matter* **1997**, *9*, 2831.
(6) Peera, A. A.; Alemany, L. B.; Billups, W. E. *Appl. Phys. a−Mater. Sci. Processing* **2004**, *78*, 995.
(7) Attalla, M. I.; Vassallo, A. M.; Tattam, B. N.; Hanna, J. V. *J. Phys. Chem.* **1993**, *97*, 6329.
(8) Dorozhko, P. A.; Lobach, A. S.; Popov, A. A.; Senyavin, V. M.; Korobov, M. V. *Chem. Phys. Lett.* **2001**, *336*, 39.
(9) Shul'ga, Y. M.; Tarasov, B. P.; Fokin, V. M.; Shul'ga, N. Y.; Vasilets, V. N. *Phys. Solid State* **1999**, *41*, 1391.
(10) Okotrub, A. V.; Bulusheva, L. G.; Asanov, I. P.; Lobach, A. S.; Shulga, Y. M. *J. Phys. Chem. A* **1999**, *103*, 716.
(11) Peera, A.; Saini, R. K.; Alemany, L. B.; Billups, W. E.; Saunders: M.; Khong, A.; Syamala, M. S.; Cross, R. J. *Eur. J. Org. Chem.* **2003**, 4140.
(12) Loufty, R. O.; Wexler, E. M. Procs. of 2001 DOE Hydrogen Prog. Rev. NREL/CP-570−30535, 2001.
(13) Tarasov, B. P.; Shul'ga, Y. M.; Fokin, V. N.; Vasilets, V. N.; Shul'ga, N. Y.; Schur, D. V.; Yartys, V. A. *J. Alloys Compds.* **2001**, *314*, 296.
(14) Shul′ga, Y. M.; Tarasov, B. P.; Fokin, V. N.; Martynenko, V. M.; Schur, D. V.; Volkov, G. A.; Rubtsov, V. I.; Krasochka, G. A.; Chapusheva, N. V.; Shevchenko, V. V. *Carbon* **2003**, *41*, 1365.
(15) Darwish, A. D.; Avent, A. G.; Taylor, R.; Walton, D. R. M. *J. Chem. Soc., Perkin Trans. 2* **1996**, 2051.
(16) Talyzin, A. V.; Shulga, Y. M.; Jacob, A. *Appl. Phys. a−Mater. Sci. Processing* **2004**, *78*, 1005.
(17) Talyzin, A. V.; Sundqvist, B.; Shulga, Y. M.; Peera, A. A.; Imus, P.; Billups, W. E. *Chem. Phys. Lett.* **2004**, *400*, 112.
(18) Talyzin, A. V.; Tsybin, Y. O.; Peera, A. A.; Schaub, T. M.; Marshall, A. G.; Sundqvist, B.; Mauron, P.; Zuttel, A.; Billups, W. E. *J. Phys. Chem. B*, submitted for publication.
(19) Talyzin, A. V.; Tsybin, Y. O.; Schaub, T. M.; Mauron, P.; Shulga, Y. M.; Zuttel, A.; Sundqvist, B.; Marshall, A. G. *J. Phys. Chem. B* **2005**, *109*, 12742.
(20) Raffaelli, A.; Saba, A. *Mass Spectrom. Rev.* **2003**, *22*, 318.
(21) Purcell, J. M.; Rodgers, R. P.; Hendrickson, C. L.; Marshall, A. G. Submitted for publication.
(22) Schaub, T. M.; Hendrickson, C. L.; Quinn, J. P.; Rodgers, R. P.; Marshall, A. G. *Anal. Chem.* **2005**, *77*, 1317.
(23) Syage, J. A. *J. Am. Soc. Mass Spectrom.* **2004**, *15*, 1521.
(24) Heiney, P. A.; Fischer, J. E.; McGhie, A. R.; Romanow, W. J.; Denenstein, A. M.; McCauley, J. P.; Smith, A. B.; Cox, D. E. *Phys. Rev. Lett.* **1991**, *66*, 2911.
(25) Bini, R.; Ebenhoch, J.; Fanti, M.; Fowler, P. W.; Leach, S.; Orlandi, G.; Ruchardt, C.; Sandall, J. P. B.; Zerbetto, F. *Chem. Phys.* **1998**, *232*, 75.
(26) Marshall, A. G.; Hendrickson, C. L.; Jackson, G. S. *Mass Spectrom. Rev.* **1998**, *17*, 1.
(27) Marshall, A. G.; Rodgers, R. P. *Acc. Chem. Res.* **2004**, *37*, 53.
(28) Ryabenko, A. G.; Muradyan, V. E.; Esipov, S. E.; Cherepanova, N. I. *Russ. Chem. Bull.* **2003**, *52*, 1516.
(29) Stoddart, M. W.; Brownie, J. H.; Baird, M. C.; Schmider, H. L. *J. Organomet. Chem.* **2005**, *690*, 3440.
(30) Moder, M.; Nuchter, M.; Ondruschka, B.; Czira, G.; Vekey, K.; Barrow, M. P.; Drewello, T. *Int. J. Mass Spectrom.* **2000**, *196*, 599.
(31) Xu, C. H.; Scuseria, G. E. *Phys. Rev. Lett.* **1994**, *72*, 669.